Chemical Science

ROYAL SOCIETY OF CHEMISTRY

EDGE ARTICLE

View Article Online
View Journal | View Issue

Cite this: *Chem. Sci.*, 2023, **14**, 8393

All publication charges for this article have been paid for by the Royal Society of Chemistry

Received 11th May 2023
Accepted 9th July 2023

DOI: 10.1039/d3sc02417b

rsc.li/chemical-science

Tetrahomo corona[4]arene-based spirophanes: synthesis, structure, and properties†

Shen-Yi Guo,[a] Zhuo-Ang Zhang,[a] Shuo Tong,*[a] Qing-Hui Guo,[b] Ruimao Hua[a] and Mei-Xiang Wang*[a]

In contrast to a plethora of macrocyclic and cage compounds, spirophanes have remained largely unexplored. We report herein the construction, structure and properties of unprecedented tetrahomo corona[4]arene-based ditopic and tritopic macrocycles of spiro structures. Synthesis was conveniently achieved by means of an efficient S_NAr reaction from simple and commercially available starting materials. Racemic samples were resolved into enantiopure chiral tetrahomo *i*-corona[4]arenes, spirophanes and bispirophanes which show interesting chiroptical properties. The acquired electron-deficient macrocyclic compounds were found to adopt unique conformational structures and to form distinct complexes with TTF in the solid state. Our study provides a new opportunity to develop multitopic macrocycles of different topologies which have potential applications in supramolecular chemistry.

Introduction

Since Lehn's pioneering work on the construction of macrotricyclic receptors to selectively recognize diammonium guests,[1] design and synthesis of ditopic and multitopic receptors have become a fast-growing research area in macrocyclic and supramolecular chemistry.[2] A plethora of ditopic and multitopic receptors consisting of functional macrocycles as binding sites have been reported. Tailor-made synthetic topologic hosts have found wide applications ranging from selective recognition of complex guests[3] and ion pairs,[4] fabrication of functional materials[5] and molecular machines,[6] structural and functional mimicking of enzymes[7] to supramolecular polymers.[8] Despite fascinating development of the field, the structures of macrocyclic ditopic and multitopic hosts are limited. Most of the macrocyclic ditopic and multitopic hosts,[1–8] for instance, are constructed by connecting platform compounds such as crown ethers,[9] cyclodextrins,[10] calixarenes[11] and their analogs[12] using spacers or tethers. Macrocyclic spirophanes, spiro molecular structures which are composed of the same or different types of macrocycles, are very rare and they have remained largely unexplored.[13]

The past decade has witnessed the emergence of a diversity of new synthetic macrocycles.[12,14] One of the interesting and useful macrocyclic hosts is corona[*n*]arenes[14g,15] and their homo corona[*n*]arene analogs.[16] They are composed of *p*-(het)arylenes and X and CH_2X (X = heteroatoms), respectively, in an alternative fashion. Substitution of *p*-(het)arylenes with *m*- or *o*-(het)arylenes results in the formation of *i*-corona[*n*]arenes and homo *i*-corona[*n*]arenes.[17] The tunable electronic features, macrocyclic geometries, and cavities obtained by the combination of various aromatic subunits and heteroatom linkages render corona[*n*]arenes and homo corona[*n*]arenes selective hosts for anions,[15–17] organic cations,[18] and electron-neutral guests.[19] Most of the corona[*n*]arenes and homo corona[*n*]arenes are readily accessible by the aromatic nucleophilic substitution reaction (S_NAr) between dinucleophiles and activated dihalogenated (het)arenes. For example, a one-pot reaction of hydroquinone and benzene-1,4-dithiol with 3,6-dichlorotetrazine in the presence of an acid scavenger affords the corresponding oxygen and sulfur-linked corona[3]arene[3]tetrazine products[20,21] while tetrahomo corona[2]arene[2]tetrazines[16] and *i*-corona[2]arene[2]tetrazines[17] are obtained from stepwise S_NAr reactions of *p*-, *m*- and *o*-dihydroxymethyl or -dimercaptomethyl benzenes with 3,6-dichlorotetrazine. We envisioned that the fragment or module coupling approach using functional group-bearing aromatic reactants would permit the synthesis of functionalized tetrahomo corona[4]arenes isomers. Further chemical manipulations and macrocyclization reactions would enable the construction of novel and interesting topological structures. We report herein the synthesis and structures of tetrahomo corona[4]arene-based spirophanes and bispirophanes. Being different from documented spirophanes

[a]*Key Laboratory of Bioorganic Phosphorus Chemistry and Chemical Biology (MOE), Department of Chemistry, Tsinghua University, Beijing 100084, China. E-mail: tongshuo@mail.tsinghua.edu.cn*

[b]*Stoddart Institute of Molecular Science, Department of Chemistry, Zhejiang University, Hangzhou, 310027, China. E-mail: wangmx@mail.tsinghua.edu.cn*

† Electronic supplementary information (ESI) available. CCDC 2261277–2261287, 2261291, 2261299, 2261294, 2261295, 2261288, 2261289, 2261298, 2261290, 2261292 and 2261293. For ESI and crystallographic data in CIF or other electronic format see DOI: https://doi.org/10.1039/d3sc02417b

bearing a spiro carbon center,[13] the topological bi- and tri-macrocyclic molecules in question contain a tetra-substituted arene as a simplified spiro superatom.[22] Alternatively, the spirophanes disclosed in the current study are indeed orthogonaphanes because of the "orthogonality" of the two adjacent macrocyclic rings.[23]

Results and discussion

Synthesis of tetrahomo i-corona[4]arenes

We commenced our study by synthesizing tetrahomo *i*-corona[4]arenes **7** by means of a fragment coupling approach. As depicted in Scheme 1, two directional *O*-alkylation reactions of perfluorohydroquinone **1a** and hydroquinone **1b** with 1,3-bis-(bromomethyl)benzene **2** under basic conditions led to the formation of intermediates **4a** and **4b**, respectively. Good yields of **4** were obtained when an excess amount of **2** (10 equiv.) was used. Decreasing the ratio of **2** over aromatic diol **1** to 3 : 1 eroded the yield of the desired product (Table S2†). In order to develop a method for the construction of tetrahomo *i*-corona[4]arenes, we systematically optimized the conditions for the macrocyclization reaction between **4a** and **6a** in terms of catalyst, base, solvent, temperature and reaction time (Table S4†). We were pleased to find out that, in the presence of tetraethylammonium bromide (TEAB) (20 mol%) as a phase transfer catalyst and K_2CO_3 (4 equiv.) as a base, refluxing **4a** with equimolar diisopropyl 2,5-dihydroxyterephthalate **6a** in a mixture of CH_3CN and THF ($v : v = 4 : 1$) afforded macrocyclic product **7a** in 66% yield. It should be noted that formation of **7a** was not observed when THF or $CHCl_3$ was employed as the reaction medium. A polar solvent such as CH_3CN appeared beneficial for the aliphatic nucleophilic substitution reaction while THF was added to dissolve substrate **6a**. The absence of a phase transfer catalyst or the replacement of TEAB with others led to a decrease in yield. Heating was necessary as the reaction did not proceed at all at ambient temperature.

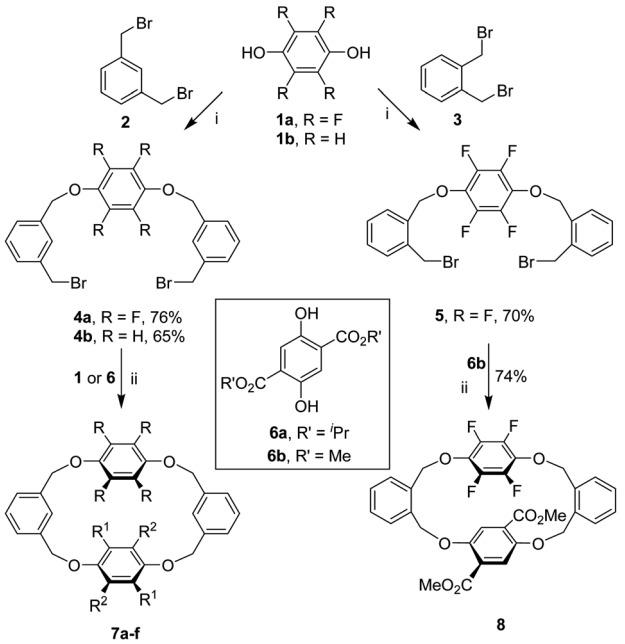

7	7a	7b	7c	7d	7e	7f
R	F	F	F	H	H	H
R^1	H	H	F	H	H	F
R^2	$CO_2{}^iPr$	CO_2Me	F	$CO_2{}^iPr$	CO_2Me	F
Yield (%)	66	69	59	40 (58)[iii]	37 (55)[iii]	27 (38)[iv]

Scheme 1 Synthesis of macrocyclic compounds **7** and **8**. i. K_2CO_3 (6 equiv.), CH_3CN/THF ($v : v = 4 : 1$), 40 °C or reflux, 2 + 0.5 h. Reactant **2** or **3** (*ca.* 8 equiv.) was recovered after the reaction; ii. TEAB (20 mol%), K_2CO_3 (4 equiv.), CH_3CN/THF ($v : v = 4 : 1$), reflux, 4 + 10 h. iii. Chemical yields were improved to 58% and 55% when TEAB (100 mol%) and K_2CO_3 (6 equiv.) were used. iv. **7f** was obtained in 38% yield from the reaction of **4a** and **1b**.

Under the optimized conditions, dibromide intermediates **4** reacted similarly with perfluorohydroquinone **1a**, hydroquinone **1b** and dimethyl 2,5-dihydroxyterephthalate **6b** to produce the corresponding tetrahomo *i*-corona[4]arenes (Scheme 1). Noticeably, the reaction of tetrafluorophenylene-containing dibromide **4a** with aromatic diols gave **7a–c** in comparable yields (59–69%). By contrast, lower chemical yields (27–40%) were obtained from the same macrocyclization reaction starting with hydroquinone-derived dibromide **4b** because of the competing oligomerization reaction between reactants. The chemical yields of **7d** and **7e** were improved to 58% and 55% when equimolar TEAB and an excess amount of K_2CO_3 were used, respectively. It is interesting to note that tetrahomo *i*-corona[4]arene **7f** was synthesized by two routes. While the reaction of **4b** with perfluorohydroquinone **1a** gave **7f** in only 27% yield along with a few unidentified by-products, the reaction between **4a** and **1b** appeared relatively clean affording macrocycle **7f** in 38% yield. These results indicated the effect of the structure of linear precursors on the macrocyclization reaction. It is most probably that the linear precursor derived from **4a** and **1b** adopts C-conformation more favourably than that from the reaction of **4b** and **1a** because, in the former case, the polar tetrafluorophenylene is located in the middle of the linear reactant. As a result, the reaction of **4a** with **1b** is more prone to macrocyclization than the reaction of **4b** with **1a** under identical reaction conditions.

The established method worked efficaciously for the construction of *o*-phenylene-bearing tetrahomo *i*-corona[4]arene **8**. For instance, alkylation of perfluorohydroquinone **1a** with 1,2-bis(bromomethyl)benzene **3** (10 equiv.) in the presence of K_2CO_3 resulted in the formation of intermediate **5** in 70% yield. Under phase transfer catalysis, the macrocyclization reaction between **5** and dimethyl 2,5-dihydroxyterephthalate **6b** proceeded efficiently to furnish the expected product **8** in 74% yield (Scheme 1). In a gram-scale synthesis, 82% yield was obtained.

Structure of tetrahomo *i*-corona[4]arenes

Prior to the construction of spirophanes, we looked at the structures of the acquired tetrahomo *i*-corona[4]arenes. All products **7** and **8** are crystalline compounds, and high quality

single crystals were cultivated by vapor diffusion of hexane or heptane into the solution of **7** or **8** in DCE, THF or ethyl acetate (Table S11†). X-ray diffraction experiments revealed various interesting conformational structures in the solid state (Fig. 1, S1, and S2†). For example, macrocyclic molecule **7c** adopts a highly symmetric conformation. Two *m*-phenylenes and *p*-perfluorophenylenes incline to the plane defined by four bridging methylene carbon atoms and by four linking oxygen atoms, respectively, forming a closed cavity. Almost the same conformational structure was observed for **7f**. Molecule **7e** exists in the pinched cone conformation in which two *m*-phenylene rings are face-to-face paralleled. By contrast, compounds **7a** and **7b** give heavily distorted partial cone conformers in the crystalline state. Due to different substitution patterns of phenylene units, macrocyclic molecule **8** adopts a conformer in which two *o*-phenylene units are located roughly in the same plane. *p*-Perfluorophenylene and dimethyl terephthalate are inclined to the plane with a dihedral angle of 49.9° and 46.6°, respectively. (Fig. S2†). The ^{1}H NMR spectra of tetrahomo *i*-corona[4]arene compounds **7** and **8** show a single set of proton signals, suggesting most probably the presence of various conformers which undergo very rapid interconversions at ambient temperature relative to the NMR time scale. Except for **7c** and **7f** which exhibited singlet proton signals of methylene moieties, geminal coupling (^2J) (a pair of doublets) was evident for methylene protons of the rest of the macrocyclic compounds indicating inequivalence of methylene protons owing to the planar chirality of the molecules.

Synthesis of spirophanes

Having two types of tetrahomo *i*-corona[4]arenes in hand, we set out to synthesize ditopic spirophanes. The pre-installed ester group on phenylene provides a versatile handle for chemical manipulations. Reduction of diesters **7e** and **8** with $LiAlH_4$ at 0 °C thus yielded diol products **9** and **10** almost quantitatively. In the presence of collidine as an acid scavenger, diols **9** and **10** underwent aromatic nucleophilic substitution reactions with 3,6-dichlorotetrazine **11** in warm 1,2-dichloroethane (DCE) to afford the corresponding products **12** and **13**. Since our attempted construction of a tetraoxa-linked tetrahomo corona[2]arene[2]tetrazine structure was not successful (Tables S8 and S9†), we turned our attention to sulfur-bridged tetrahomo corona[2]arene[2]tetrazine. To our delight, the macrocyclization reaction of both **12** and **13** with equimolar 1,4-phenylenedimethanethiol **14** under basic conditions proceeded efficiently at ambient temperature in DCM. Spirophanes **15** and **16** consisting of both a tetrahomo corona[2]arene[2]tetrazine and a tetrahomo *i*-corona[4]arene were obtained in 74% and 71% yield, respectively (Scheme 2).

Encouraged by the successful construction of spirophanes **15** and **16**, we sought to synthesize bispirophanes. With the aim of obtaining a sulfur-linked tetrahomo corona[2]arene[2]tetrazine core, diol-bearing cyclophanes **9** and **10** were converted to dithiol compounds. As illustrated in Scheme 3, reactions of diols **9** and **10** with NBS with the aid of PPh_3 produced dibromides **17** and **18** in 73% and 60% yield, respectively. (Table S10†) Further treatment with ethanethioic S-acid (AcSH) followed by alcoholysis with methanol led to dithiol products nearly quantitatively. The aromatic nucleophilic substitution reaction of the resulting dithiols **19** and **20** with 3,6-dichlorotetrazine **11** took place smoothly in the presence of DIPEA to afford good yield of 6-chloro-*s*-tetrazine-appended macrocycles **21** and **22**.

Having had the necessary building blocks at hand, we first attempted the reaction of macrocyclic dithiols **19** with intermediate **21** (Scheme 4). Theoretically, macrocyclization *via*

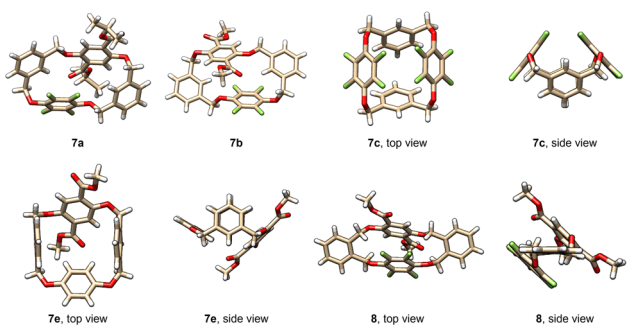

Fig. 1 X-ray molecular structures of **7** and **8**.

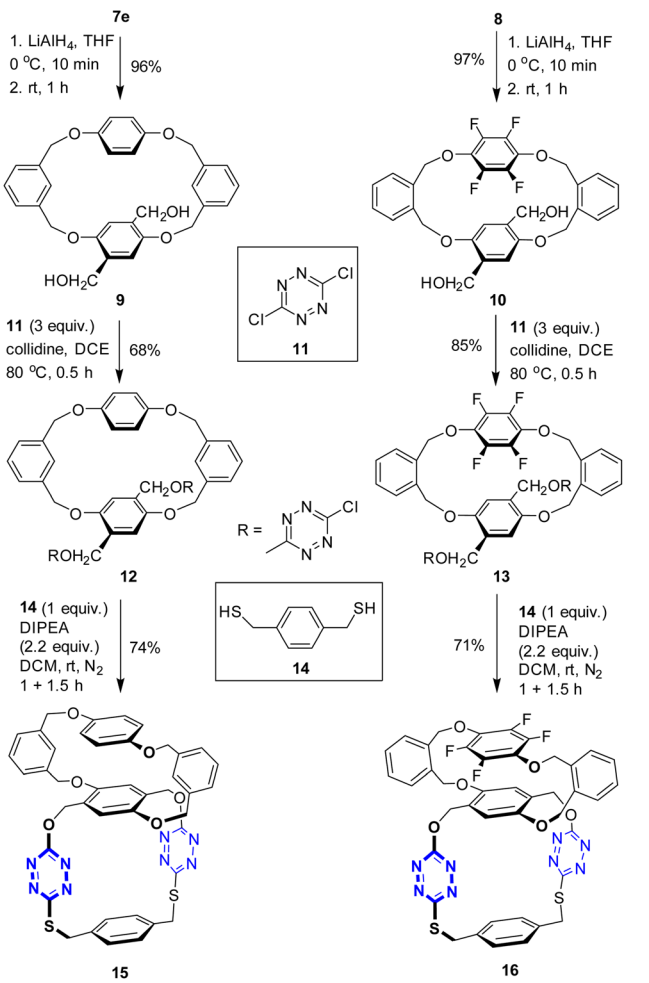

Scheme 2 Synthesis of ditopic spirophanes **15** and **16**.

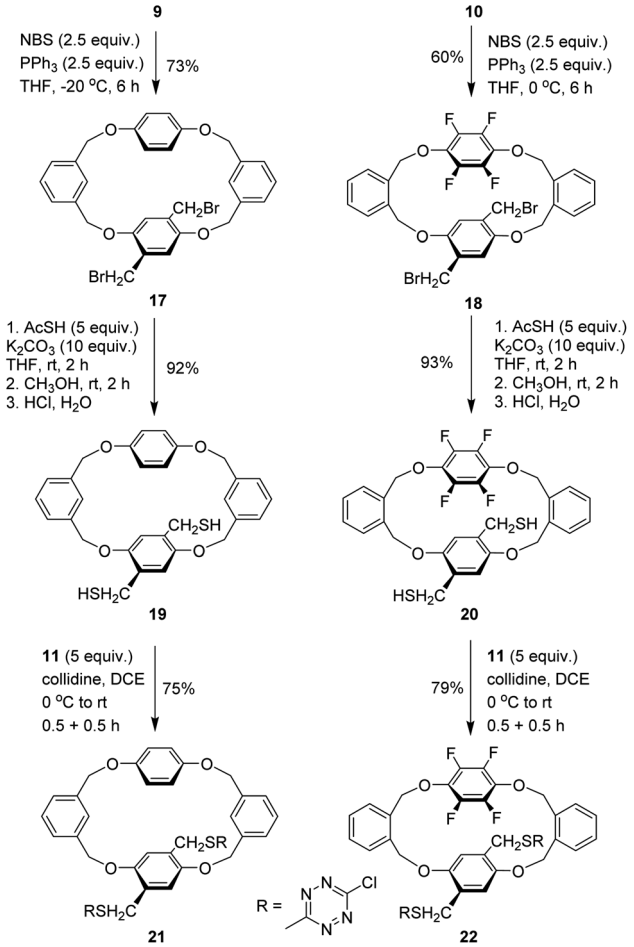

Scheme 3 Preparation of intermediates 19–22.

double S_NAr reactions would lead to the formation of meso bispirophane **23a** and racemic bispirophane **23b**. Under the same basic conditions as those for the synthesis of spirophanes **15** and **16**, the reaction between **19** and **21** proceeded smoothly at ambient temperature. From the reaction mixture, racemic bispirophane compound (±)-**23b**, which was resolved into a pair of enantiomers (*vide infra*), was isolated as the sole macrocyclic product in 20% yield. The meso compound **23a** was not obtained. Intriguingly, high diastereoselectivity was also observed in the reaction of **19** with building block **12**. Racemic compound

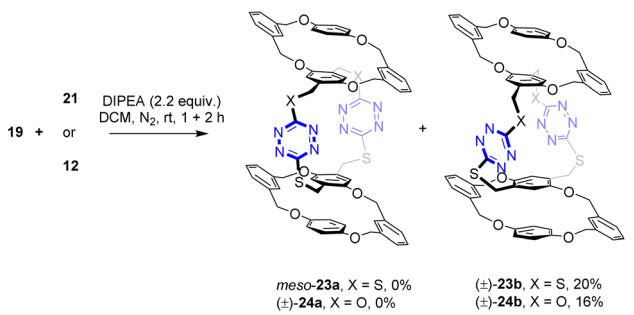

Scheme 4 Synthesis of bispirophanes 23 and 24.

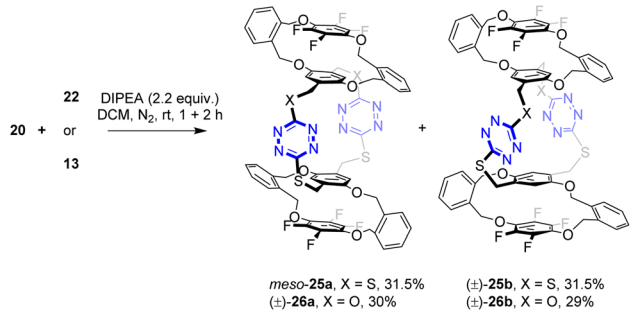

Scheme 5 Synthesis of bispirophanes 25 and 26.

(±)-**24b** was delivered as the major product while the pseudo-meso compound (±)-**24a** was not formed.

(±)-**24a** was not formed (Scheme 4). In contrast to *m*-phenylene-containing building blocks (Scheme 4), the analogous macrocyclization reaction between *o*-phenylene-bearing tetrahomo *i*-corona[*n*]arenes **20** and **22** or **13** afforded a mixture of diastereomers *meso*-**25a** and (±)-**25b** or (±)-**26a** and (±)-**26b** in good yields. The diastereomeric ratio, which was readily measured by ^{1}H NMR spectroscopy, was 1 : 1, suggesting that the formation of these bispirophanes was not selective. It is most likely that the molecular rigidity of *o*-dihydroxymethylbenzene-derived tetrahomo *i*-corona[4]arenes enables the high efficiency of the construction of bispirophanes but with low diastereoselectivity (Scheme 5). Diastereomers (±)-**26a** and (±)-**26b** were separated by means of preparative thin-layer chromatography. The meso-**25a** and (±)-**25b** were not separable chromatographically because of the same polarity. Fortunately, the later compound was obtained as high-quality single crystals from recrystallization of a mixed sample in toluene and hexane. It may be worth noting that bispirophanes **25a** and **25b** were also prepared in a 1 : 1 ratio from the direct reaction of **20** with 3,6-dichlorotetrazine **11** albeit in 12% yield (ESI).

Structure of spirophanes

The spiro and bispiro structures, which were determined unambiguously by the X-ray crystallography method as racemic products **15**, **16**, **25b** and **26** are crystalline and formed high quality single crystals readily from recrystallization (Table S11†), as depicted in Fig. 2, S3, and S4.† A brief glimpse of the X-ray molecular structures depicted in Fig. 2 shows clearly that the spirophanes in question contain orthogonally aligned adjacent macrocyclic cavities. It is evident that there is a pair of *P*- and *M*-enantiomers of **15** in the crystal structure. While tetrahomo corona[2]arene[2]tetrazine moieties in both spirostructures adopt similar partial cone conformations, the conformation of tetraoxa tetrahomo *i*-corona[4]arene sub-macrocycles in the two enantiomers varies however. One gives a partial cone (Fig. 2A) while the other forms a slightly twisted 1,3-alternate (Fig. 2B). Because of the *o*-substitution pattern of phenylene, the tetrahomo *i*-corona[4]arene sub-ring in spirophane **16** is heavily distorted in the solid state (Fig. 2C). Noticeably, macrocyclic conformation of tetrahomo *i*-corona[4]arene sub-moieties in bispirophanes **25b** (Fig. 2D), **26a** (Fig. 2E) and **26b** (Fig. 2F) remains analogous. The

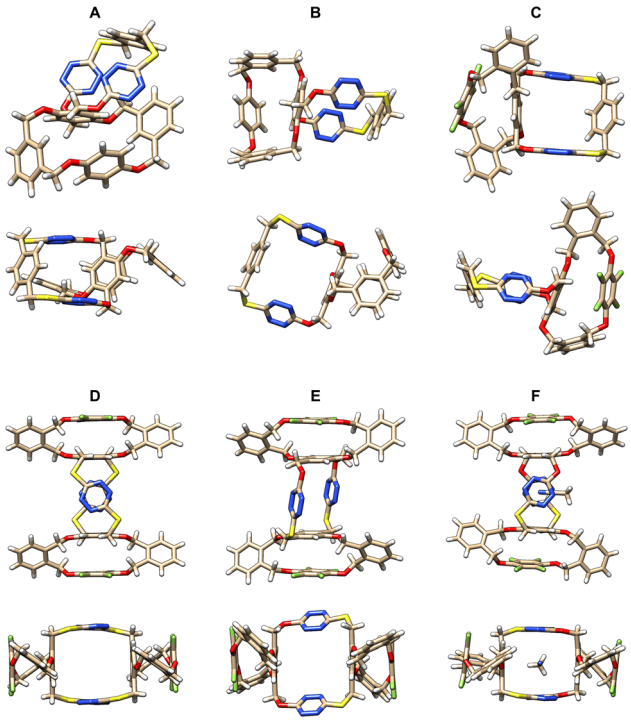

Fig. 2 X-ray molecular structures of racemic spirophanes **15** (A and B) and **16** (C) and bispirophanes **25b** (D), **26a** (E) and **26b** (F) with top and side views or two different side views.

tetrafluorophenylene ring is face-to-face aligned with the tetrasubstituted phenylene ring with a centroid distance of 3.5–3.6 Å. Two distal *o*-phenylene rings in **25b** and **26a** tend to be perpendicular with a dihedral angle of around 70° (Fig. S4A and B†). In the case of **26b**, dihedral angles of 72° and 45° are observed (Fig. S4C†). Tetrahomo corona[2]arene[2]tetrazines of **25b** and **26b** adopt the same conformation in which two tetrazine rings and two phenylene rings are face-to-face paralleled irrespective of the heteroatom linkages. They form a very similar box-like cavity (Fig. 2D and F). However, the centroid distance between tetrazine rings in S_4-linked macrocycle **25b** (6.71 Å) is slightly larger than that of O_2, S_2-bridged macrocycle **26b** (6.38 Å). Because of varied bond connectivity, macrocyclic conformation of tetrahomo corona[2]arene[2]tetrazine in **26a** differs considerably from that of **25b** and **26b**. Evidently, two tetrasubstituted phenylene rings are orthogonal to the plane defined by four bridging heteroatoms. Two paralleled tetrazine rings are inclined to the plane with a dihedral angle of 42° (Fig. 2E and S4B†).

It is worth addressing that during the recrystallization from a mixture of 1,2-dichloroethane and methanol, bispirophane **25b** can complex $[H_3O]^+Cl^-$ available in solvent. The X-ray molecular structure shows that, in the electron-deficient cavity of tetrahomo corona[2]arene[2]tetrazine, a chloride ion is sandwiched comfortably by tetrazine rings due to anion-π noncovalent bond interactions[24] (Fig. S5†). By contrast, an acetonitrile molecule is included in the central cavity of **26b** owing to size complementarity and dual lone-pair electron-π (lpe-π) interactions[25] between guest and electron-deficient tetrazines (Fig. 2F).

Complexation with tetrathiafulvalene

The spirophanes and bispirophanes acquired would provide ditopic and tritopic macrocyclic host molecules for the study of molecular recognition and self-assembly. The observation of the spontaneous formation of complexes of the tetrahomo corona[2]arene[2]tetrazine moiety with chloride and acetonitrile prompted us to explore the interaction of spirophanes with electron-rich tetrathiafulvalene (TTF). It was found that compounds **15** and **16** formed complexes readily with TTF in solution to give single crystals. Interestingly, the use of different conditions led to different host–guest complexes. For example, hexane vapor diffusion into a mixture of racemic **16**, TTF in THF and 1,4-dioxane at ambient temperature resulted in the formation of brown-colored crystals. However, black crystals were obtained from the vapor diffusion of hexane into a solution of racemic **16** and TTF in chloroform at −20 °C. X-ray diffraction analysis of a brown-colored single crystal revealed that in the crystal structure there are a pair of enantiomers of **16**, two TTF molecules and one 1,4-dioxane molecule (Fig. 3 left and Fig. S6†) while in a black crystal there are a pair of enantiomers of **16** complexed with four TTF and two $CHCl_3$ molecules (Fig. 3 right and Fig. S8†). Each tetrahomo corona[2]arene[2]tetrazine ring of *P*- and *M*-enantiomers in both cases adopts partial cone conformation and complexes one five-membered ring of the TTF molecule *via* lpe-π interaction and C–H···$N_{tetrazine}$ hydrogen bonding. Notably, the other five-membered ring of the included TTF forms multiple hydrogen bonds with another host **16** molecule of the same planar chirality (Fig. 3). In the former case, one-dimensional assemblies of $[TTF\cdot(P\text{-}\mathbf{16})]_n$ and $[TTF\cdot(M\text{-}\mathbf{16})]$ are aligned alternatively (Fig. S6 and S7†). By contrast, layer-by-layer assemblies of $[TTF\cdot(P\text{-}\mathbf{16})]_n$ and $[TTF\cdot(M\text{-}\mathbf{16})]$ in an alternative manner were observed in the latter case. In addition, in each layer, another TTF molecule is located in between tetrazine rings of the neighbouring spirophane by forming sandwich-type π–π interactions (Fig. S8†).

On the other hand, in stark contrast to **16**, racemic **15** forms a complex with TTF in a completely different manner. As revealed by X-ray crystallography, both *P*- and *M*-enantiomers form conformational structures in which tetrahomo *i*-corona[4]arene and corona[2]arene[2]tetrazine adopt a partial cone and cone, respectively (Fig. 4). This bispiro macrocyclic conformation in complex varies remarkably from that of the parent **15** (Fig. 2A and

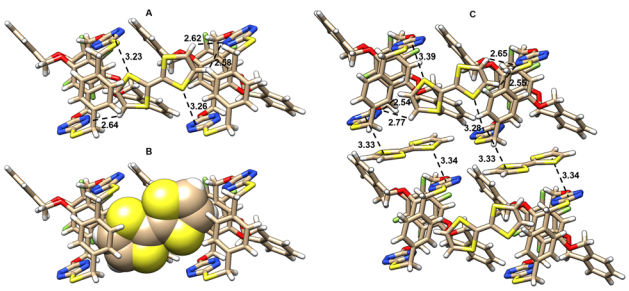

Fig. 3 X-ray molecular structures of complexes between racemic **16** and TTF obtained at room temperature (left) and at −20 °C (right) with side views. Solvent molecules are omitted for clarity.

B). Through C–H/π and hydrogen bond interactions, each *P*- and *M*-tetrahomo corona[2]arene[2]tetrazine cavity includes a TTF molecule. Their partial cone tetrahomo corona[4]arene moieties interact with another two TTF molecules by means of π/π, C–H/π and hydrogen bonding interactions (Fig. 4). Most interestingly, *P*- and *M*-configured tetrahomo corona[2]arene[2]tetrazine-bonded TTF molecules undergo π–π stacking interaction to form a heterochiral capsule-like complexing motif (Fig. 4). In the meantime, TTF molecules bonded to tetrahomo *i*-corona[4]arene of either *P*- or *M*-conformation undergo association with the neighbouring macrocycles to form a heterochiral capsule-like assembly. In other words, the interaction between racemic **15** and TTF led to the formation of an infinite one-dimensional assembly consisting of a [*P*-**15**$\cdots$(TTF)$_2\cdots$*M*-**15**$\cdots$(TTF)$_2\cdots$*P*-**15**$\cdots$(TTF)$_2\cdots$*M*-**15**]$_n$ repeating unit in the solid state (Fig. S9†).

Enantiopure spirophanes and chiroptical properties

As we have already stated, some tetrahomo *i*-corona[4]arenes, spirophanes and dispirophanes are planar chiral compounds. To shed light on their chiroptical properties, we resolved successfully racemic compounds **7a**, **7d**, **8**, **15**, **16**, **23b**, **24b** and **26** into pairs of enantiomers by means of the HPLC method with columns coated with a chiral stationary phase (Table S13 and Fig. S15–S30†). High quality single crystals of the enantiopure compounds *P*-**7d**, *M*-**15**, *P*,*M*-**26a** and *P*,*P*-**26b** were cultivated (Table S11†) and their absolute configurations were determined beyond any doubt. Noteworthily, molecular structures of *P*-**7d**, *M*-**15** and *P*,*M*-**26a** (Fig. S10–S12†) in the solid state resemble those of their racemic compounds (Fig. 1 and 2). However, in contrast to the X-ray molecular structure of racemic **26b** (Fig. 2F), the tetrazine-bearing macrocycle within bispirophane enantiomer *P*,*P*-**26b** adopts cone conformation with two tetrahomo *i*-corona[4]arene macrocycles tending to be perpendicular to each other (Fig. S13†).

Prior to the study of chiroptical properties of chiral macrocycles and spirophanes, electronic spectra of racemic samples were measured. UV-visible spectra of tetrahomo *i*-corona[4]arenes **7a**, **7b**, **7d**, **7e** and **8** in CH_3CN, DCM and toluene showed a maximum absorption band (λ_{max}) centered at 328 nm–334 nm with a molar absorption coefficient (ε) of (3.5–5.7) $\times$ 10^3 L mol^{-1}cm^{-1} (Fig. S31 and Table S14†). Due to the presence of a dialkyl 2,5-dialkoxyterephthalate chromophore, under the irradiation of UV light (λ_{ex} = 330 – 340 nm), they emitted strong fluorescence (λ_{em}) at 402–420 nm in toluene with quantum yield (ϕ) ranging from 61.5% to 69.4%. Interestingly, the quantum yield of **7d** and **7e** decreased dramatically to below 5% when their emission spectra were recorded in DCM and CH_3CN, whereas photophysical properties of **7a** and **7b** were not sensitive to the nature of the solvent used (Fig. S32†). In CH_3CN, all compounds which contain a tetrazine moiety exhibited a characteristic n $\rightarrow$ π* absorption band of tetrazine at 513–514 nm (**12**, **13**, **21**, and **22**) or 523–525 nm (**15**, **16**, **23**, **24**, and **26**) with ε = (1.0–1.7) $\times$ 10^3 L mol^{-1} cm^{-1} in addition to strong absorption bands at short wavelengths. Spiro and bispiro macrocycles were weakly fluorescent (λ_{em} = 571–573 nm, ϕ < 2%) when they were irradiated with UV light (λ_{ex} = 330–340 nm) (Fig. S33 and Table S14†).

The electronic circular dichroism (ECD) spectra of enantiopure products were measured in CH_3CN. As depicted in Fig. 5, pairs of enantiomers of tetrahomo *i*-corona[4]arenes **7a**, **7d** and **8** gave complementary ECD spectra. *P*- and *M*-enantiomers of tetrahomo *i*-corona[4]arenes **7a**, **7d**, and **8** showed weak positive and negative Cotton effects at 325–335 nm with anisotropy dissymmetry factors $|g_{abs}|$ of (1.8–2.6) $\times$ 10^{-3}. Perfect mirror-image ECD spectra of spirophanes **15** and **16** and bispirophanes **23b**, **24b**, **26a** and **26b** were also observed (Fig. 5). In accordance with UV-visible spectra, positive and negative Cotton effects of tetrazine chromophores of *M*- and *P*-spirophanes **15** and **16** and bispirophanes appeared at 517–531 nm. The $|g_{abs}|$ factors of spirophanes and bispirophanes were in the range of (1.0–2.0)$\times$$10^{-3}$ except for the enantiomers of **26a** which gave a smaller $|g_{abs}|$ value (5.0 $\times$ 10^{-4}) because they have a pseudo meso-structure, *viz.* the chirality of **26a** stems from

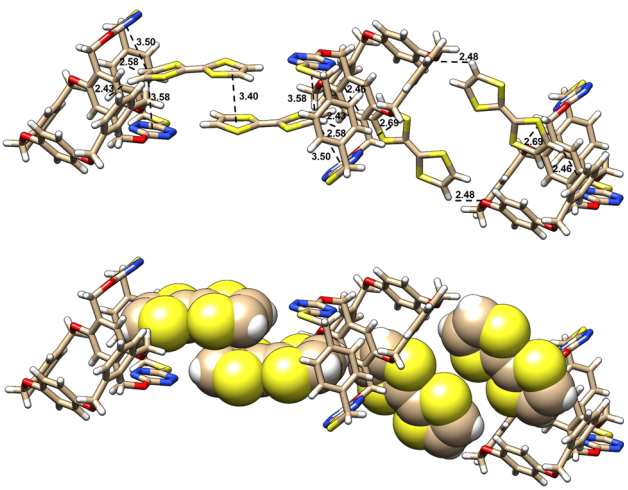

Fig. 4 X-ray molecular structures of complexes between racemic **15** and TTF with side views. Solvent molecules are omitted for clarity.

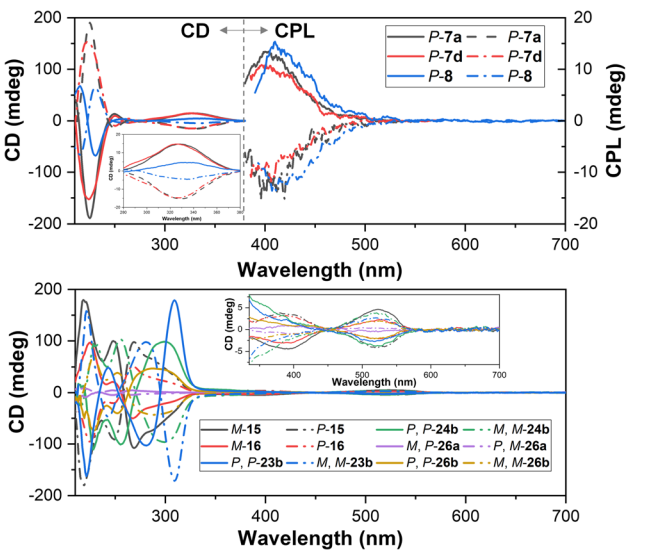

Fig. 5 The electronic circular dichroism and circularly polarized luminescence spectra of tetrahomo *i*-corona[4]arenes **7a**, **7d**, and **8** in acetonitrile (CD) and toluene (CPL) (top) and the electronic circular dichroism spectra of spirophanes **15** and **16** and bispirophanes **23b**, **24b**, and **26** in acetonitrile (bottom).

the difference between oxygen and sulfur linking atoms within the central macrocyclic subunit. It is also noteworthy that enantiomers of tetrahomo *i*-corona[4]arenes **7a**, **7d** and **8** emitted complementary circularly polarized luminescence (CPL) at λ = 400–420 nm with the anisotropy dissymmetry factors ($|g_{lum}|$) being around 0.002. The CPL properties along with high quantum yield would render tetrahomo *i*-corona[4]arenes a potential platform for further development of macrocyclic CPL materials. Unfortunately, enantiopure spirophanes **15** and **16** and bispirophanes **23b**, **24b** and **26a** and **26b** were not CPL active both in solution and in the solid state.

Conclusions

In conclusion, we have developed a convenient method to synthesize a diversity of novel tetrahomo *i*-corona[4]arenes, spirophanes and bispirophanes from simple and commercially available starting materials based on the S_NAr reaction. Spirophanes and bispirophanes contain adjacent macrocyclic rings or cavities which are orthogonally orientated. Resolution of racemic samples affords enantiopure chiral tetrahomo *i*-corona[4]arenes, spirophanes and bispirophanes which show interesting chiroptical properties. The acquired macrocyclic compounds adopt unique conformational structures and form distinct complexes with TTF in the solid state. Our study provides a new strategy to construct multitopic macrocycles of different topologies which may have potential applications in the recognition of complex guests and the construction of self-assembled functional materials.

Data availability

The authors declare that the data supporting the findings of this study are available within the paper and the ESI, as well as from the authors upon request.

Author contributions

S. Y. G., S. T., R. M. H., Q. H. G., and M. X. W. conceived and designed the experiments. S. Y. G. and Z. A. Z. carried out the experiments. S. Y. G., S. T., and M. X. W. wrote the manuscript. All authors contributed to the reviewing and editing of the manuscript and ESI.†

Conflicts of interest

There are no conflicts to declare.

Acknowledgements

We thank the National Natural Science Function of China (22193020, 22193022, 21821001, 21920102001, and 22050005) and Tsinghua University for financial support.

Notes and references

1 F. Kotzyba-Hibert, J. M. Lehn and P. Vierling, *Tetrahedron Lett.*, 1980, **21**, 941–944.
2 J. L. Atwood, G. W. Gokel and L. J. Barbour, in *Comprehensive Supramolecular Chemistry II*, Elsevier, Amsterdam, 2017.
3 For a recent review, see: G. Mamardashvili, N. Mamardashvili and S. Koifman, *Molecules*, 2021, **26**, 5292.
4 For selected reviews, see: (*a*) S. K. Kim and J. L. Sessler, *Chem. Soc. Rev.*, 2010, **39**, 3784–3809; (*b*) A. J. McConnell, A. Docker and P. D. Beer, *ChemPlusChem*, 2020, **85**, 1824–1841.
5 For a recent example, see: Z.-Y. Li, Y. Zhang, C.-W. Zhang, L.-J. Chen, C. Wang, H. Tan, Y. Yu, X. Li and H.-B. Yang, *J. Am. Chem. Soc.*, 2014, **136**, 8577–8589.
6 For a fascinating example, see: J. D. Badjić, V. Balzani, A. Credi, S. Silvi and J. F. Stoddart, *Science*, 2004, **303**, 1845–1849.
7 For selected examples, see: (*a*) J. Yang and R. Breslow, *Angew. Chem., Int. Ed.*, 2000, **39**, 2692–2695; (*b*) R. Cacciapaglia, A. Casnati, L. Mandolini, A. Peracchi, D. N. Reinhoudt, R. Salvio, A. Sartori and R. Ungaro, *J. Am. Chem. Soc.*, 2007, **129**, 12512–12520.
8 For a recent review, see: T. Haino, *Polym. J.*, 2019, **51**, 303–318.
9 G. Gokel, in *Crown Ethers and Cryptands*, Royal Society of Chemistry, Cambridge, 1991.
10 G. Crini, *Chem. Rev.*, 2014, **114**, 10940–10975.
11 D. Gutsche, in *Calixarenes – An Introduction*, Royal Society of Chemistry, Cambridge, 2nd edn, 2008.
12 P. Neri, J. Sessler and M.-X. Wang, in *Calixarenes and Beyond*, Springer, Cham, 2016.
13 (*a*) T. A. Schaub, E. A. Prantl, J. Kohn, M. Bursch, C. R. Marshall, E. J. Leonhardt, T. C. Lovell, L. N. Zakharov, C. K. Brozek, S. R. Waldvogel, S. Grimme and R. Jasti, *J. Am. Chem. Soc.*, 2020, **142**, 8763–8775; (*b*) G. A. Consiglio, S. Failla and P. Finocchiaro, *J. Phys. Org. Chem.*, 2004, **17**, 760–768; (*c*) G. Hohlneicher, D. Bremm, J. Wytko, J. Bley-Escrich, J.-P. Gisselbrecht, M. Gross, M. Michels, J. Lex and E. Vogel, *Chem.–Eur. J.*, 2003, **9**, 5636–5642; (*d*) A. McAuley, S. Subramanian, M. J. Zaworotko and K. Biradha, *Inorg. Chem.*, 1999, **38**, 5078–5085.
14 (*a*) X.-N. Han, Y. Han and C.-F. Chen, *Chem. Soc. Rev.*, 2023, **52**, 3265–3298, DOI: **10.1039/d3cs00002h** and references cited therein;; (*b*) Z.-Y. Zhang and C. Li, *Acc. Chem. Res.*, 2022, **55**, 916–929; (*c*) J.-R. Wu, G. Wu and Y.-W. Yang, *Acc. Chem. Res.*, 2022, **55**, 3191–3204; (*d*) L.-P. Yang, X. Wang, H. Yao and W. Jiang, *Acc. Chem. Res.*, 2020, **53**, 198–208; (*e*) P. D. Sala, R. D. Regno, C. Talotta, A. Capobianco, N. Hickey, S. Geremia, M. De Rosa, A. Spinella, A. Soriente, P. Neri and C. Gaeta, *J. Am. Chem. Soc.*, 2020, **142**, 1752–1756; (*f*) W. Yang, K. Samanta, X. Wan, T. U. Thikekar, Y. Chao, S. Li, K. Du, J. Xu, Y. Gao, H. Zuilfoh and A. C.-H. Sue, *Angew. Chem., Int. Ed.*, 2020, **59**, 3994–3999; (*g*) M.-X. Wang, *Sci. China: Chem.*, 2018, **61**, 993–1003; (*h*) T. Ogoshi, T.-a. Yamagishi and Y. Nakamoto, *Chem. Rev.*, 2016, **116**, 7937–8002.
15 For recent examples, see: (*a*) S.-Y. Guo, Q.-H. Guo, S. Tong and M.-X. Wang, *Angew. Chem., Int. Ed.*, 2020, **59**, 8078–8083; (*b*) M.-D. Gu, Y. Lu and M.-X. Wang, *J. Org. Chem.*, 2020, **85**, 2312–2320.

16 H.-B. Liu, Q. Zhang and M.-X. Wang, *Angew. Chem., Int. Ed.*, 2018, **57**, 6536–6540.
17 S.-Y. Zhuang, Y. Cheng, Q. Zhang, S. Tong and M.-X. Wang, *Angew. Chem., Int. Ed.*, 2020, **59**, 23716–23723.
18 (*a*) M.-Y. Zhao, Q.-H. Guo and M.-X. Wang, *Org. Chem. Front.*, 2018, **5**, 760–764; (*b*) Q.-H. Guo, L. Zhao and M.-X. Wang, *Angew. Chem., Int. Ed.*, 2015, **54**, 8386–8389.
19 W.-S. Ren, L. Zhao and M.-X. Wang, *Org. Lett.*, 2016, **18**, 3126–3129.
20 Q.-H. Guo, Z.-D. Fu, L. Zhao and M.-X. Wang, *Angew. Chem., Int. Ed.*, 2014, **53**, 13548–13552.
21 Q.-H. Guo, L. Zhao and M.-X. Wang, *Chem.–Eur. J.*, 2016, **22**, 6947–6955 and references cited therein.
22 According to IUPAC, bicyclic phanes with one tetrasubstituted aromatic ring are named spirophanes because a tetrasubstituted aromatic ring is simplified as a spiro superatom. For an example, see: *Nomenclature of Organic Chemistry, IUPAC Recommendations and Preferred Names 2013*, International Union of Pure and Applied Chemistry, RSC, 2014, p. 313, or **https://iupac.qmul.ac.uk/BlueBook/**, P-2, p. 134.
23 The authors of this paper are grateful to one of the referees for proposing orthogonaphane as a general name for the synthetic compounds.
24 For a recent review of anion-π non-covalent interactions, see: D.-X. Wang and M.-X. Wang, *Acc. Chem. Res.*, 2020, **53**, 1364–1380.
25 A. Bauzá, T. J. Mooibroek and A. Frontera, *ChemPlusChem*, 2015, **16**, 2496–2517.